Regenerative pulsations in semiconductor etalon due to competition between carrier generation and heating effects on band filling

Regenerative pulsations in semiconductor etalon due to competition between carrier generation and heating effects on band filling

Valery I. Tolstikhin[a)]
Faculty of Electrical Engineering, Telecommunication Technology and Electromagnetics, Eindhoven University of Technology, P.O. Box 513, 5600 MB Eindhoven, The Netherlands

Alexander V. Grigor'yants
Institute of Radio Engineering and Electronics of the Russian Academy of Sciences, 11 Mokhovaya, 103907 Moscow, Russia

Theo G. van de Roer
Faculty of Electrical Engineering, Telecommunication Technology and Electromagnetics, Eindhoven University of Technology, P.O. Box 513, 5600 MB Eindhoven, The Netherlands

(Received 2 December 1996; accepted for publication 27 May 1997)

Competition between carrier concentration and effective temperature effects on the dielectric function of a degenerate semiconductor in a spectral range near its fundamental absorption edge is suggested as a mechanism for regenerative pulsations in a stationary pumped optical etalon. The origin of self-pulsations is similar to that in a bistable etalon with competing concentration and thermal optical nonlinearities, but, due to its purely electronic nature, the proposed mechanism provides a way for a much higher repetition frequency, probably in the GHz range. The model of the phenomenon and modeling examples are all related to a Fabry–Perot resonator filled with the bulk n^+- $In_{0.53}Ga_{0.47}As$ as an active medium. © *1997 American Institute of Physics.* [S0021-8979(97)02817-X]

I. INTRODUCTION

It is well known, that a stationary pumped optical bistable device can be made to pulsate, provided its overall optical nonlinearity (ON) results from two competing mechanisms with considerably different time-constants.[1] Although this is quite a common phenomenon, not restricted by any particular type of device nor mechanism of ON, most foregoing studies,[2–7] including ours,[4–7] refer to a semiconductor etalon with electronic and thermal dispersive nonlinearities. In that case, carrier concentration, due to band filling in a narrow band gap semiconductor like InSb[3–7] or weakening of free-exciton resonance in a wide band gap semiconductor like GaAs,[2] and lattice temperature both effect the near absorption edge refractive index, but in opposite manners. The former plays the role of the fast variable responsible for optical bistability, while slow variation of the latter prevents either state from being stable, that ultimately results in the regenerative oscillations. An ability of such a system to selfpulsate has been shown experimentally,[2,3] in particular, monostable pulse generation and multiple oscillatory mode regime in a stationary pumped InSb etalon have been observed.[6,7] The characteristic frequency of the regenerative oscillations, limited by a relaxation of the slower variable, in a semiconductor etalon with the competing electronic and thermal nonlinearities, is determined by the lattice cooling time and usually lies in a range below 1 MHz. In fact, these are too low frequencies for application in all-optical clock systems,[8] pulse generators,[9] etc. Increase of the frequency within the same scheme of regenerative oscillations requires that the slow thermal ON is replaced by a faster one. Here, carrier heating combined with carrier generation under the band filling conditions are suggested as alternative pair of the competing *purely electronic* mechanisms of ON, assuming that carrier cooling is a much faster process than carrier recombination. The frequency of self-pulsations is then determined by the carrier lifetime which provides a way for increasing it toward the GHz range.

II. MODEL OF A SEMICONDUCTOR ETALON

Bearing in mind the prospects of the future utilization, consider the epitaxial Fabry–Perot resonator formed by a heavily doped $n^+In_{0.53}Ga_{0.47}As$ layer grown on a quarter-wave stack of alternative SiO_2–Si layers, as a dielectric bottom mirror.[10] With the upper surface of a semiconductor layer or another quarter-wave stack as a top mirror, the device operates in a reflection mode [see insertion in Fig. 3(b)]. Let this semiconductor etalon be stationary and uniformly pumped with a monochromatic radiation at a frequency ω corresponding to interband transitions into the states below the Fermi level, assumed to be well above the bottom of the conduction band. Light absorption results from the direct interband and indirect (impurity, carrier, and phonon assistant) intraband transitions, which effect both the concentration and energy distribution of the charge carriers. Since the interband absorption is reduced by the band filling, optical generation is relatively weak and, hence, the electron concentration, N_e, does not differ significantly from its dark value, equal to the concentration of donors, N_0, while the hole concentration, N_h, is low as compared to these two. High concentration of free carriers assures quasineutrality, i.e., N_e, N_0, and N_h are connected by the equation: $N_e = N_0 + N_h$. Also due to the high concentration, electrons can be considered as

[a)]On leave from the Institute of Radio Engineering and Electronics of the Russian Academy of Sciences, 11 Mokhovaya, 103907 Moscow, Russia. Electronic mail: v.i.tolstikhin@ele.tue.nl

thermalized on all the actual time scales and so their energy distribution is characterized by the effective temperature, T_e, different from the crystal temperature, T_0, assumed constant.[11] Heavy holes, contrary to light electrons, are supposed to be in the equilibrium with the crystal lattice and they are described by the temperature T_0. Distribution of N_h and T_e along the axis of the vertical cavity is nearly homogeneous, provided damping of the light beam in a single pass through the semiconductor layer is weak, while the hole diffusion and electron thermal conductivity lengths both are long compared to the period of a standing lightwave. We assume these conditions are met. Moreover, in this article we restrict ourselves by considering only the homogeneous distributions also in the plane of the semiconductor layer, leaving the transversal effects[4,5] to an additional study. Then, the description of the semiconductor etalon is reduced to the following two rate equations:

$$\frac{dN_h}{dt}=\alpha_{cv}\eta\frac{I_i}{\hbar\omega}+G-R, \tag{1}$$

$$\frac{dW_e}{dt}=(\alpha_{cv}\Delta_{cv}+\alpha_c\Delta_c)\frac{\eta I_i}{\hbar\omega}+Q-P. \tag{2}$$

Here, W_e is the density of electron energy, α_{cv} and α_c are the coefficients of the interband and intra (conduction) band absorption, Δ_{cv} and Δ_c are the characteristic energies yielded in the electron gas as a result of a single event of the interband and intraband absorption; η is the ratio of the internal light intensity, averaged over the cavity, to the intensity of incident radiation, I_i; G, and Q are the carrier and energy generation rates apart from the optical pump, R and P are the rates of hole recombination and electron energy relaxation, respectively. Generally, stimulated emission in a spectral range below ω but above $\varepsilon_g/\hbar$, where ε_g is the band gap of a semiconductor material, also can contribute to the rates of change in the carrier concentration and density of energy, provided the inversion of carrier population, caused by the optical pump, results in a gain of the resonator modes that compensates their radiation losses. However, assuming the cavity length as reasonably short and hence the radiation losses as too high, in the present study we neglect stimulated emission effects.

All the values in Eqs. (1) and (2), except with I_i, should be expressed in terms of N_h (N_e) and T_e. This requires that certain assumptions are made with respect to the band structure, light-carrier interaction, and charge carrier relaxation processes.

For the band structure, a simple two parabolic band model that accounts only for the central Γ-valley electrons and heavy holes is used throughout. Thus, the electron density of energy is determined by $W_e=1.5T_e\aleph_c\Phi_{3/2}(\xi_e)$, where $\aleph_c(T_e)$ is the temperature-dependent density of states in the conduction band, $\Phi_{3/2}$ is the Fermi–Dirac integral of the order 3/2, and ξ_e is the electron chemical potential, normalized to the effective temperature, T_e, hereafter measured in the energy units. ξ_e is related to N_e and T_e as $N_e=\aleph_c(T_e)\Phi_{1/2}(\xi_e)$. By using this equation, the derivative dW_e/dt is expressed as

$$\frac{dW_e}{dt}=\psi_T T_e\frac{dN_e}{dt}+\psi_N N_e\frac{dT_e}{dt}, \tag{3}$$

where

$$\psi_T=1.5\Phi_{1/2}(\xi_e)/\Phi_{-1/2}(\xi_e)$$

and

$$\psi_N=1.5\ [2.5\Phi_{3/2}(\xi_e)/\Phi_{1/2}(\xi_e)-\psi_T].$$

For the direct interband transitions, taking into account free-carrier screening of the Coulomb interaction and considering only the spectral range above $\varepsilon_g/\hbar$, excitonic effects are neglected and the absorption coefficient α_{cv} is then given by a single-particle approximation:

$$\alpha_{cv}=A_{cv}\left[\frac{\varepsilon_g}{\hbar\omega}\left(1-\frac{\varepsilon_g}{\hbar\omega}\right)\right]^{1/2}[1-f_e(\varepsilon_e)-f_h(\varepsilon_h)]. \tag{4}$$

Here, A_{cv} is a normalization constant, proportional to the squared matrix element of momentum, $f_j(\varepsilon_j)=[1+\exp(\varepsilon_j T_j-\xi_j)]^{-1}$ is the occupation probability for electron ($j=e$) and hole ($j=h$) states at the energy $\epsilon_j=(\mu_{eh}/m_j)(\hbar\omega-\varepsilon_g)$, where m_j, $j=e,h$ is the effective mass of electron or heavy hole and $\mu_{eh}=(1/m_e+1/m_h)^{-1}$ is the reduced effective mass of the electron-hole pair. The energy Δ_{cv} in Eq. (2) is then equal to the energy of photogenerated electrons, ε_e.

Regarding the indirect intraband transitions, their contribution to the optical absorption, as computed by the second-order perturbation theory, is a result of summation over the relevant mechanisms of electron scattering. By taking into account the impurity, heavy hole and LO-phonon scattering, the coefficient of intraband absorption can be written down as[12,13]

$$\alpha_c=\frac{\aleph_c(T_e)}{\sqrt{2\pi}}\int_0^\infty\frac{du\,u}{(u+u_s)^2}\times\ln\left\{\frac{1+\exp[\xi_e+\delta-(u+\delta^2u^{-1})/2]}{1+\exp[\xi_e-\delta-(u+\delta^2u^{-1})/2]}\right\}\times(\sigma_I\delta^{1/2}+\sigma_{\mathrm{LO}}\delta^{-1/2}u). \tag{5}$$

Here, u_s is a parameter that accounts for free-carrier screening; $\delta=\hbar\omega/2T_e$; $\sigma_I\propto N_e(\hbar\omega)^{-7/2}$ and $\sigma_{\mathrm{LO}}\propto(\hbar\omega)^{-5/2}$ are the characteristic absorption cross-sections related to the impurity—heavy hole and LO-phonon contributions, respectively. In the limit of a high optical frequency and strong degeneracy, $\delta\gg\xi_e\gg1$ and $\delta\gg u_s$, Eq. (5) reduces to $\alpha_c=(\sigma_I+\sigma_{\mathrm{LO}})N_e$. The total absorption coefficient $\alpha=\alpha_{cv}+\alpha_c$ is given by the sum of expressions (4) and (5). The latter is written down within an accuracy of $\Omega/\omega\ll1$, where Ω is the LO phonon frequency, which allows one to assume $\Delta_c\approx\hbar\omega$ in Eq. (2).

Due to a strong frequency dispersion, in the spectral range near the fundamental absorption band, any variations of α are reflected in the variations of the refractive index n and a corresponding change in the propagation constant, $\beta=n\omega/c$. So far as in our model the absorption coefficient is a function of the carrier concentrations and effective temperature and does not depend on the optical field directly, the

conventional Kramers–Kronig transformation can be used to connect variations of β and α, produced by change in N_h, N_e, and T_e:

$$\delta\beta=\frac{\pi}{\omega}P\int_0^\infty \frac{d\omega'}{\omega'^2-\omega^2}[\alpha(\omega',N_h,N_e,T_e) - \alpha(\omega',0,N_0,T_0)]-\frac{2\pi e^2 N_h}{n_0\mu_{eh}\omega c}, \tag{6}$$

where the last term, with n_0 as the lattice refractive index, takes into account the plasma effect.

Concerning the description of the radiation inside the cavity, by assuming the inequalities $\alpha d \ll 1 \ll \beta d$, where d is the thickness of the semiconductor layer, we use the mean field approximation which results in the following relationships for the earlier introduced parameter, η, and the net reflectivity of the etalon, ρ:[14]

$$\eta=\frac{[\exp(\alpha d/2)+\rho_b\exp(-\alpha d/2)](1-\rho_t)}{[\exp(\alpha d/2)-\sqrt{\rho_t\rho_b}\exp(-\alpha d/2)]^2+4\sqrt{\rho_t\rho_b}\sin^2(\phi_0+\delta\beta d)} \tag{7}$$

$$\rho=\frac{[\sqrt{\rho_t}\exp(\alpha d/2)-\sqrt{\rho_b}\exp(-\alpha d/2)]^2+4\sqrt{\rho_t\rho_b}\sin^2(\phi_0+\delta\beta d)}{[\exp(\alpha d/2)-\sqrt{\rho_t\rho_b}\exp(-\alpha d/2)]^2+4\sqrt{\rho_t\rho_b}\sin^2(\phi_0+\delta\beta d)}, \tag{8}$$

where ϕ_0 is the initial (dark) phase, considered as a given parameter, ρ_t and ρ_b are the reflection coefficients of the top and bottom mirrors, respectively.

Generation apart from the optical pump, which in fact is the thermal generation, plays no role in a heavily doped semiconductor and, therefore, it is ignored; i.e., $G=0$. Among the possible recombination mechanisms, the most important in a narrow band gap semiconductor like InGaAs with a very high concentration of electrons and relatively low concentration of holes, is the CHCC Auger process in which two electrons and one heavy hole are involved, with a recombination rate given by[15]

$$R\approx C\frac{\Phi_{3/2}(\xi_e)}{\Phi_{1/2}(\xi_e)}\frac{T_e}{T_0}N_e^2N_h, \tag{9}$$

where C is the characteristic constant, normalized to the equilibrium temperature. Every event of the CHCC Auger recombination results in a rise of the energy of the electron gas amounting to the band gap energy, ε_g. This process is considered here as the only mechanism for energy generation apart from the optical pump and, hence, $Q=\varepsilon_g R$.

The last thing to be defined with respect to Eqs. (1) and (2) is the rate of the electron energy relaxation, P. It is assumed to be caused mostly by the inelastic LO-phonon scattering that is typical for the polar III-V semiconductors.[16] Then, as is clear from the experimental data[17] and theoretical studies,[18] including ours,[19] nonequilibrium phonon effects play an important role in cooling of the high-density electron gas. This is due to the intensive generation of LO-phonons by hot electrons, which disturbs the equilibrium phonon distribution and ultimately results in a relaxation of the coupled hot electron-LO-phonon system as a single whole. On a time scale longer than the LO-phonon spontaneous emission time, around 0.1–0.2 ps, the energy relaxation rate, which takes into account both the free-carrier screening and phonon nonequilibrium effects, is[19]

$$P=\frac{\hbar\Omega}{\tau_\Omega}(f_{\Omega e}-f_{\Omega 0})\left(\frac{\hbar\Omega}{\pi T_e}\right)^{1/2}\aleph_c(T_e)\int_0^\infty\frac{duu}{(u+u_s)^2} \times\ln\left[1+\frac{f_e(\varepsilon_\Omega)}{f_{\Omega e}}\right]\frac{\nu_{\Omega D}}{\nu_{\Omega D}+\nu_{\Omega E}}. \tag{10}$$

Here, τ_Ω is the characteristic relaxation time; $f_{\Omega e}=[\exp(\hbar\Omega/T_e)-1]^{-1}$, $f_{\Omega 0}=[\exp(\hbar\Omega/T_0)-1]^{-1}$, and $f_e(\varepsilon_\Omega)=[\exp(\varepsilon_\Omega/T_e-\xi_e)+1]^{-1}$, where $\varepsilon_\Omega=\hbar\Omega(u+1)^2/4u$; $\nu_{\Omega E}$ and $\nu_{\Omega D}$ are the LO-phonon emission and decay frequencies, respectively, the former defined as

$$\nu_{\Omega E}=\frac{1}{\tau_\Omega}\frac{T_e}{2\hbar\Omega}u^{-3/2}\ln\left[1+\frac{f_e(\varepsilon_\Omega)}{f_{\Omega e}}\right] \tag{11}$$

and the latter assumed constant, i.e., independent of the parameters of the electron gas.

Finally, Eqs. (1)–(11) provide the fully self-contained description of the optically pumped semiconductor etalon. The relevant numerical parameters of the band structure and carrier-phonon–photon interactions, used in the further modeling, all correspond to the bulk n^+-$In_{0.53}Ga_{0.47}As$ and they are taken from Refs. 16 and 20. In Secs. III–V, the suggested mechanism for competing electronic nonlinearities, fast optical bistability and regenerative oscillations in the semiconductor etalon are discussed on the basis of this model.

III. MECHANISM OF COMPETING NONLINEARITIES

Under the assumed excitation condition, ON of a semiconductor medium results from a dependence of its dielectric function on the carrier concentration and effective temperature, which two are subject to change with a variation of the optical field. This is the parametrical kind of nonlinearity, since it is seen only through the change of the parameters of the medium, $N_h(N_e)$ and T_e [further, $N_h(N_e)$- and T_e- related ONs are referred as the concentration and temperature nonlinearities, respectively].

The computed spectra of the change in the interband absorption coefficient, $\delta\alpha_{cv}=\alpha_{cv}(\omega,N_h,N_e,T_e)-\alpha_{cv}(\omega,0,N_0,T_0)$, and related change in the propagation

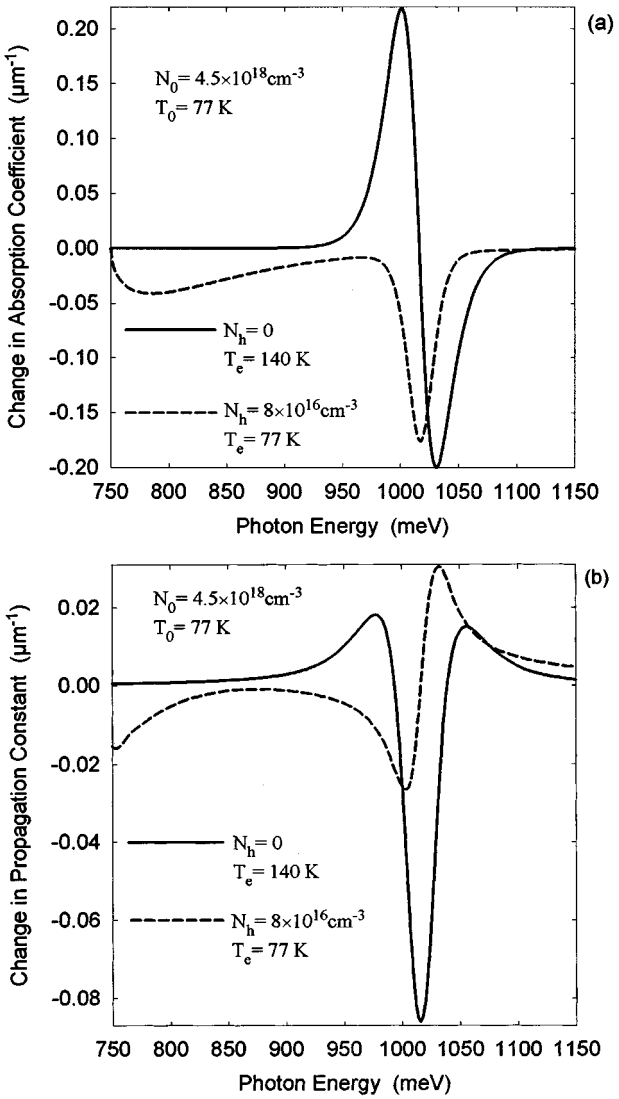

FIG. 1. Spectra of the change in (a) interband absorption coefficient and (b) related carrier contribution to the propagation constant in the bulk n^+-$In_{0.53}Ga_{0.47}As$, both caused by the variations of the electron effective temperature and hole (electron) concentration referred to the dark state: $N_h=0$, $N_e=N_0$, and $T_e=T_0$.

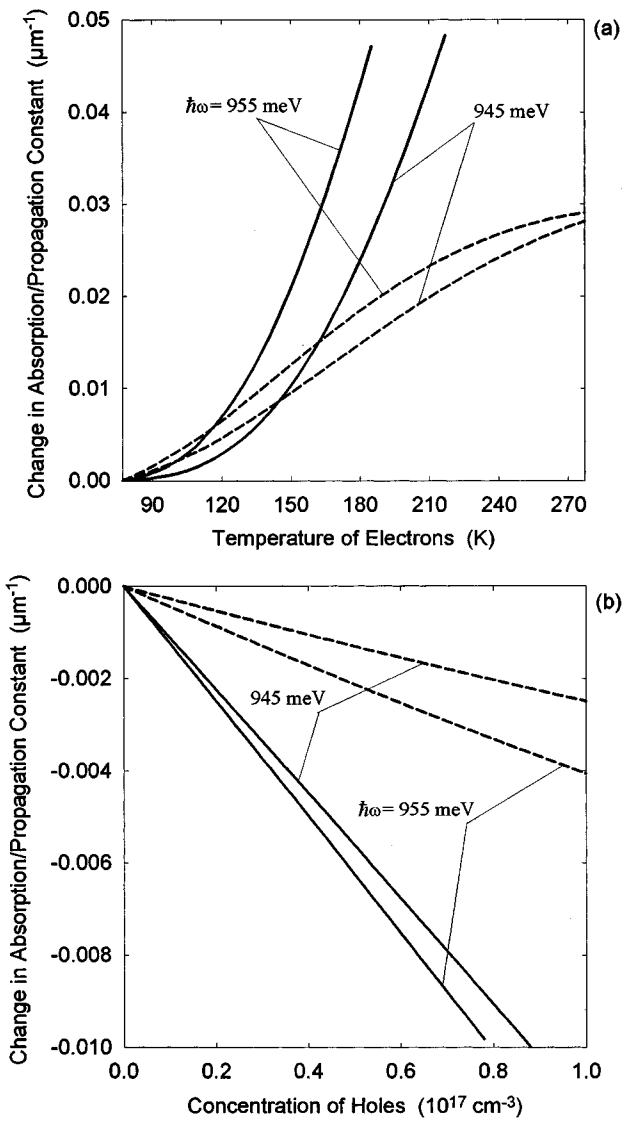

FIG. 2. Change in the interband absorption coefficient (solid lines) and related carrier contribution to the propagation constant (dashed lines) in the bulk n^+-$In_{0.53}Ga_{0.47}As$, referred to the dark state ($N_h=0$, $N_e=N_0$, and $T_e=T_0$), as the functions of (a) electron temperature and (b) hole concentration.

constant, $\delta\beta_{cv}$, caused by the variations of $N_h(N_e)$ and T_e, are shown in Fig. 1. As is seen from the plots, the carrier concentration and temperature influences upon both the $\delta\alpha_{cv}$ and $\delta\beta_{cv}$ are completely different; that is attributed to the opposite effects of $N_h(N_e)$ and T_e on the band filling.[21] Actually, the interband absorption in a degenerate semiconductor in a spectral region corresponding to the direct transitions below the Fermi level is reduced by the band filling, which is known as a Burstein–Moss effect.[22] Increase of the carrier concentration enhances the band filling and, hence, reduces the interband absorption further [dashed line in Fig. 1(a)]. In contrast, a rise of the carrier temperature suppresses the band filling, via a redistribution of the electrons toward the higher energy states, resulting in increase of α_{cv} below the Fermi level and decrease of α_{cv} above the Fermi level [solid line in Fig. 1(a)]. Corresponding changes in the propagation constant [given in Fig. 1(b) also in dashed and solid lines] just reflect the changes in the interband absorption coefficient, according to the Kramers–Kronig transformation (6). The computed temperature and concentration dependencies of the $\delta\alpha_{cv}$ and $\delta\beta_{cv}$ under the Burstein–Moss effect conditions are given in Fig. 2. It is seen that a reasonable growth of the electron temperature is capable of drastically increasing the interband absorption, initially almost completely suppressed by the band filling, which also results in a considerable rise of the propagation constant [Fig. 2(a)]. At the same time, a relatively small increase of the carrier concentration provides a way for a nearly linear decrease of both the interband absorption coefficient and propagation constant [Fig. 2(b)].

In the optically pumped semiconductor etalon, either T_e and $N_h(N_e)$ are increased due to the light-carrier interaction within the cavity. So, optical heating is caused by a release of a certain energy as a result of every event of the interband or intraband absorption, which is accounted by the

first term on the right-hand side of Eq. (2). Generally, the interband absorption is a process much more probable than the intraband absorption, since the latter is the second-order indirect (impurity or phonon assistant) process. However, under the Burstein–Moss effect conditions, the interband absorption is reduced and, therefore, the intraband absorption can dominate, especially in the carrier heating [also, this is due to the fact that $\Delta_c \sim \hbar\omega$ is a considerably higher energy than $\Delta_{cv} \sim (\mu_{eh}/m_e)(\hbar\omega - \varepsilon_g)$: assuming $\hbar\omega = 950$ meV, one gets $\Delta_{cv}/\Delta_c = 0.2$ in a case of the $In_{0.53}Ga_{0.47}As$]. If, then, the temperature mechanism of nonlinearity prevails and it is explained as follows: The relatively weak intraband absorption heats up the electron gas and, therefore, suppresses the band filling, which eventually results in a switching on the much stronger interband absorption, and hence, a drastic rise of the total absorption coefficient, $\alpha = \alpha_c + \alpha_{cv}$.[12,23] Such an absorptive ON is immediately reflected in a corresponding dispersive ON, and thus, the resulted temperature nonlinearity is a combination of the two. Note, that although the increasing absorption due to the intraband optical heating is itself capable of resulting in a resonatorless bistability, the associated dispersive ON is more efficient in the sense it provides a way to the lower threshold resonator bistability.[12] Then, optical generation, caused by the interband transitions and accounted by the first term on the right-hand side of Eq. (1), is subject to increase with a rise of the electron effective temperature. As soon as the interband absorption is switched on, the concentration nonlinearity becomes increasingly important and it appears as a decrease of the interband, and hence, the total, absorption coefficient, as well as the propagation constant, with an increase of the optical pump. Thus, optical heating and generation effects on the band filling, resulting in a reversible darkening and bleaching, respectively, are the competing purely electronic mechanisms of the ON under the Burstein–Moss effect conditions.

IV. FAST OPTICAL BISTABILITY

The temperature and concentration ONs have essentially different relaxation rates, determined by the electron cooling time, $\tau_T = N_e(\partial P/\partial T_e)^{-1}$ and the hole lifetime, $\tau_N = (\partial R/\partial N_h)^{-1}$, respectively. In the vicinity of the equilibrium state related to the modeling examples given in Figs. 1 and 2, $\tau_T \approx 1$ ps and $\tau_N \approx 1$ ns. The difference is big enough to distinguish the fast (governed by the relaxation of T_e) and slow (caused by the relaxation of N_h) stages in the dynamics of a nonlinear etalon and then on a time scale above τ_T, but well below τ_N, consider the nonequilibrium hole concentration as a given parameter. Note that a considerable difference in the relaxation rates of the competing ONs, resulting in a splitting of the fast and slow stages in the dynamics of the nonlinear system, is a general condition for a discussed kind of regenerative pulsations.[1–9] In the fast stage, the response of the semiconductor etalon is determined only by the effective electron temperature T_e which, computed as a function of the intensity of the incident light, I_i, is shown in Fig. 3(a). In this modeling example, the initial (dark) state of the etalon is slightly shifted from the resonance, assuming that a reasonable increase of the electron temperature compensates the phase shift. So far as the heating of the electron gas is caused by the absorption of light, T_e rises as the intracavity intensity of radiation grows. The latter is achieved by approaching the resonance condition, $\psi_0 + \delta\beta d = 0$, and hence, increase of the effective electron temperature leads to a growth of the intracavity light intensity and further carrier heating. If the positive optical feedback, caused by the cavity, is sufficiently strong, this results in a fast optical bistability with a switching time of the order of τ_T.[12,23] Corresponding S-shaped characteristics of T_e as the function of I_i, in which intermediate state with $dT_e/dI_i < 0$ is unstable, are shown in Fig. 3(a). Optical response (in reflected signal) of the bistable etalon is displayed in Fig. 3(b).

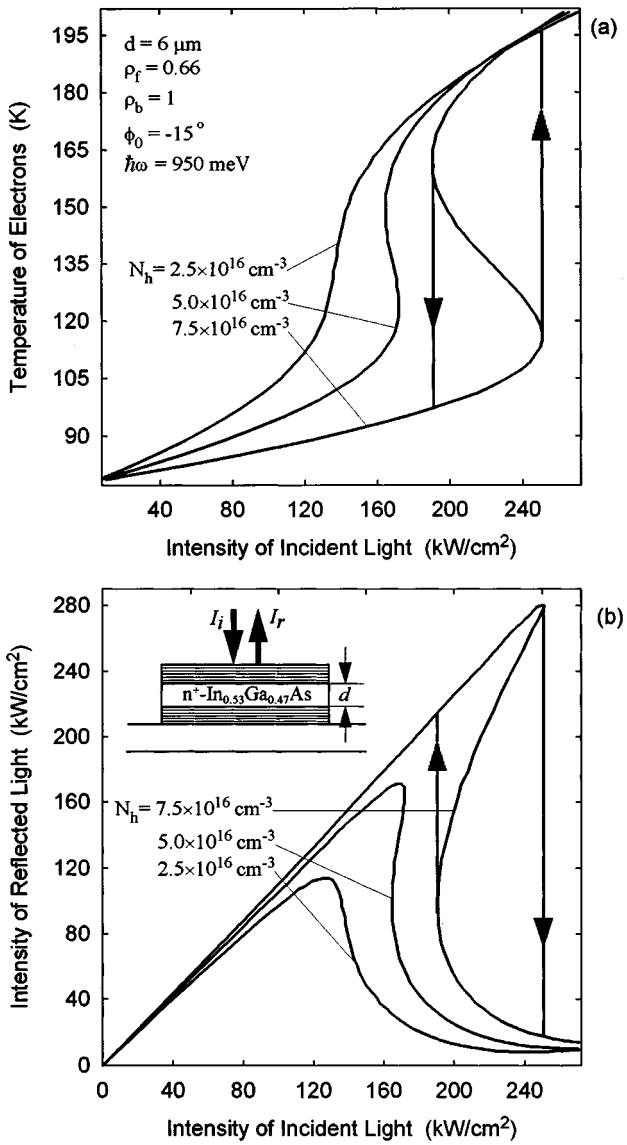

FIG. 3. Carrier heating induced bistability of the stationary pumped n^+-$In_{0.53}Ga_{0.47}As$ etalon: (a) electron temperature and (b) intensity of the reflected light as the functions of intensity of the incident light. Equilibrium (dark) state of the semiconductor medium is assumed the same as in Figs. 1 and 2.

The hole concentration is taken here as a given parameter, which, physically, reflects the fact that it remains nearly constant on a time scale of establishing the electron tempera-

ture and intracavity optical field, resulting in the bistable characteristics presented in Figs. 3(a) and 3(b). However, the hole (electron) concentration is slowly changed, due to the weak interband generation/recombination, and, as it is seen from Fig. 3, even a small variation of N_h in a range well below N_0 changes the stationary characteristics of the semiconductor etalon drastically. Rise of the hole concentration becomes apparent in two ways: (1) *via* a shift of the etalon resonance, due to a reduction of the refractive index of the semiconductor medium, and (2) through an increase of the etalon finesse, as a result of a reduction of the damping caused by the interband absorption. As a result, the device is monostable at lower and bistable at higher N_h, i.e., it exhibits threshold behavior with respect to the hole concentration. In the given numerical example, this threshold is about 4×10^{16} cm^{-3}. Above the threshold, growth of N_h shifts the hysteresis loops in both $T_e(I_i)$ and $I_r(I_i)$ characteristics toward the higher intensities of the incident light and makes them wider. At a sufficiently high hole concentration, coefficient α_{cv} changes the sign, i.e., the interband absorption is changed into the interband gain, and, should the combination $\alpha_{cv}(\hbar\omega-\varepsilon_g)/\hbar\omega+\alpha_c$ change its sign, optical heating is switched to the optical cooling. However, an optically cooled semiconductor has a quasistationary state, i.e., a state which remains nearly constant on the time scales below τ_N, only up to a certain, quite low, light intensity, limited by a recombination heating.

V. REGENERATIVE OSCILLATIONS

Change in the hole concentration causes the bistable regions in both T_e and I_r as the functions of I_i to slowly move, always in the direction of switching. In fact, suppose that a stationary pumped semiconductor etalon is in the *on* state. Then, the intracavity light intensity, ηI_i, and the effective electron temperature, T_e, take their maximum values. Carrier generation, the stronger the higher T_e, increases the finesse of the etalon and simultaneously shifts its resonance, making the bistable region move slowly toward the higher I_i. Once the lower intensity boundary of the hysteresis loop crosses the actual pumping level, the etalon is quickly switched to the *off* state, so that the intracavity intensity of light and the electron temperature both reach their minimum values, while the hole concentration remains nearly constant. The interband generation is now relatively weak or even changed into the stimulated recombination, resulting in a reduction of the hole concentration, approaching the resonance and lowering the etalon finesse, which eventually moves the bistable region toward the lower I_i. As soon as the higher intensity boundary of the hysteresis loop crosses the actual value of I_i, the etalon is quickly switched back to the *on* state. This is a repeated process which, as was pointed out first by McCall,[1] results in the self-pulsations of a stationary pumped etalon at a frequency determined by the slower relaxation process, i.e., in our case by the recombination of holes.

Oscillatory behavior of the etalon with the competing concentration and temperature nonlinearities can be analyzed by investigating a phase plane (N_h, T_e) of the rate Eqs. (1) and (2). Following a general scheme,[24] the null-clines of Eqs. (1) and (2) [further referred as the null-clines (1) and (2), respectively] are to be found; then, the stability of the steady state(s), determined as the intersection(s) of the null-clines, is to be investigated and should any one be unstable, the existence of a limit circle surrounding this intersection point has to be examined.

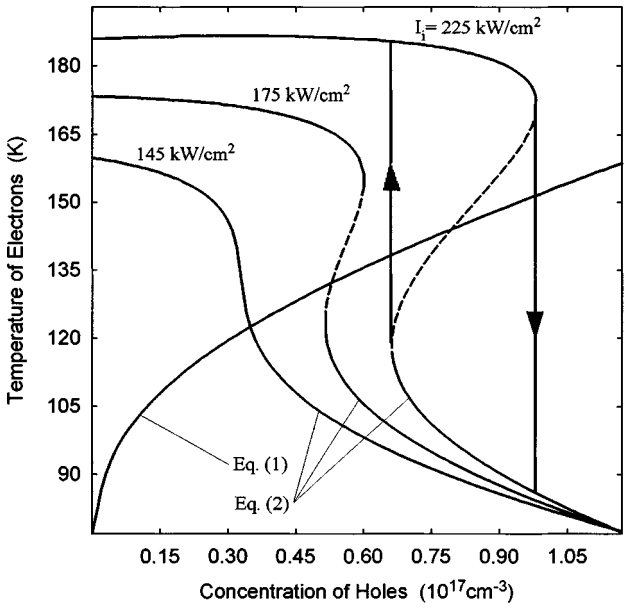

FIG. 4. Phase portrait of the dynamic system described by Eqs. (1) and (2). Dashed sections on the null-clines (2) correspond to their unstable branches. Directions of switching in the regenerative oscillation regime are shown by arrows. Parameters of the etalon are the same as in Figs. 1–3.

The computed null-clines (1) and (2) are given in Fig. 4. It is seen, that despite having a similar structure, which reflects a balance between the optical generation of carriers [Eq. (1)] or energy [Eq. (2)], on one hand, and carrier recombination or energy relaxation, on the other hand, in the phase plane (N_h, T_e) these two equations behave differently. So, within some range of the intensities of the incident light, the null-cline (1) practically does not depend on I_i and remains single-valued, while the null-cline (2) depends on I_i strongly and becomes multi-valued at intensities higher than some threshold intensity. The physics behind this difference can be clarified by rewriting the stationary Eqs. (1) and (2) in a form as

$$\alpha_{cv}(N_h, T_e) = \hbar\omega \frac{N_h}{\tau_N} \frac{1}{\eta I_i}, \tag{12}$$

$$\alpha_c(T_e) + \frac{\hbar\omega - \varepsilon_g}{\hbar\omega} \alpha_{cv}(N_h, T_e) = \left(\Delta T_e \frac{N_e}{\tau_T} - \varepsilon_g \frac{N_h}{\tau_N} \right) \frac{1}{\eta I_i}, \tag{13}$$

and taking into account that under the actual conditions the hole concentration N_h, the splitting of the electron temperature, $\Delta T_e = T_e - T_0$, the characteristic hole lifetime, τ_N, and the electron cooling time, τ_T, satisfy an inequality:

$$\frac{\tau_T}{\tau_N} \frac{N_h}{N_e} \frac{\hbar\omega}{\Delta T_e} \ll 1. \tag{14}$$

Then, it is seen that as the intensity of the incident light, I_i, increases, the null-clines (1) and (2) approach T_e as the functions of N_h, which diminish $\alpha_{cv}(N_h,T_e)$ and $\alpha_c(T_e)+[(\hbar\omega-\varepsilon_g)/\hbar\omega]\alpha_{cv}(N_h,T_e)$, respectively. At sufficiently high intensities, the null-clines are, therefore, independent of I_i and they correspond to no optical generation of carriers [Eq. (1)] or energy [Eq. (2)]. However, due to the inequality (14), there is a certain range of I_i, determined by the device parameters and/or operational conditions, where Eq. (12) can be replaced with $\alpha_{cv}(N_h,T_e)\approx 0$, but the right-hand side of Eq. (13) still cannot be neglected. Within this range, the null-cline (1) is governed only by the frequency of the incident light, remaining a single-valued, monotonous curve independent of I_i, while the null-cline (2) may be quite sensitive to the changes in I_i, especially in the etalon with a high finesse. The latter is determined, under the equal conditions, by the interband absorption coefficient, α_{cv}, which decreases and may even become negative as N_h rises, resulting in enhancement of the finesse and, at intensities higher than the threshold intensity, making the null-cline (2) multivalued.

In the given numerical example, the threshold intensity, I_{th}, is around 155 kW/cm^2 and, disregarding whether $I_i < I_{th}$ or $I_i > I_{th}$, there is only one intersection between two null-clines, corresponding to the only singular point of the dynamic system described by Eqs. (1) and (2). Linear analysis of these equations in the vicinity of the singular point, performed numerically, shows that this is actually a *node* singular point, which is a *stable node* below the threshold and *unstable node* above the threshold, provided the intersection point corresponds to $dT_e/dN_h > 0$ on the null-cline (2) (dashed sections in Fig. 4). In the first case, a stationary pumped etalon responds also stationary, while in the second case it has no stationary state at all.

To analyze the phase trajectories of the dynamic system described by Eqs. (1) and (2) in the case of the unstable singular point, we make use of the huge difference between the T_e- and N_h-relaxation times (τ_T is about three orders less than τ_N), and distinguish the fast and slow motions in the plane (N_h,T_e). On the time scales above τ_T, the electron temperature follows adiabatically the hole concentration, so that the phase trajectory $[N_h(t),T_e(t)]$ is close to the null-cline (2). This is the slow motion which, however, is possible as far as the state of an etalon, described by the stationary Eq. (2), remains stable with respect to the fast variations of the electron temperature. Only branches of the null-cline (2) corresponding to $dT_e/dN_h < 0$ (solid sections in Fig. 4) are stable, and should the initial mapping point lie outside these, it reaches one of the stable branches in a time about τ_T. This is the fast motion and it corresponds to the phase trajectories almost parallel to T_e-axis, where N_h remains nearly constant (vertical lines marked by arrows, in Fig. 4). Thus, a discontinuous limit cycle consisting of the slow motion over the stable branches of the null-cline (2), and fast switching between them at the points where derivative dT_e/dN_h changes the sign, arises, provided the only singular point of the considered system corresponds to $dT_e/dN_h < 0$, i.e., null-clines (1) and (2) intersect each other as it is shown in Fig. 4. So far as the null-cline (1) corresponds to $\alpha_{cv}(N_h,T_e)=0$, only a part of the limit cycle above this null-cline is associated with the interband absorption, $\alpha_{cv} > 0$, while the part below the null-cline (1) is related to the interband gain, $\alpha_{cv} < 0$. Hence, in a periodic motion over the limit cycle, generation of the extra carriers is changed into their stimulated recombination and vice versa.

According to a general theory,[24] presence of the limit cycle in the phase portrait of a dynamic system of the second order is the required and sufficient condition for its self-oscillations, which, in our case, appear as the periodic pulsations of a stationary pumped etalon. The period of these self-pulsations is estimated as the time of the slow motion over the limit cycle, and it is determined by the relaxation of the hole concentration after the fast switching of the electron temperature. The period can be varied, to some extent, by tuning the parameters of the semiconductor etalon, as well as the frequency and intensity of the optical pump, and, ultimately, it can be reduced up to τ_N, i.e., the frequency of self-oscillations can be enhanced toward the GHz range. Taking into account that the phase portrait of the system under consideration is qualitatively similar to that of an etalon with the competing concentration and thermal mechanisms of ON, some analogies in the nonlinear dynamics of these two systems could be expected as well. So, phenomena like the soft and sudden onsets of the self-oscillations; single-shot and periodic generation of the optical pulses; hysteresislike transitions between different oscillatory modes, all studied with respect to the etalon with competing concentration and thermal mechanisms of ON (Refs. 2–7 and 9), probably have to appear also in the etalon with the purely electronic mechanisms of ON, but on much shorter time scales.

VI. CONCLUSIONS

In conclusion, a novel physical mechanism of the competing optical nonlinearities, resulting in the regenerative oscillations of a bistable semiconductor etalon, is proposed and theoretically studied. The electronic nature of both the competing nonlinearities provides a way for having these oscillations at a high frequency. Under the actual practice conditions, the period of self-oscillations is limited by the Auger recombination time in a heavily degenerate n-type semiconductor, which enables one to increase the frequency of regenerative oscillations toward the GHz range. The ability to obtain the optical pulses at GHz repetition frequencies from a (quasi)stationary pumped device makes the bistable semiconductor etalon with the competing electronic nonlinearities a promising element for applications in all-optical digital systems.

ACKNOWLEDGMENTS

This work was supported by The International Science Foundation, Grant No. M8K300 and The Russian Foundation for Basic Research, Grant No. 96-02-18395.

[1] S. L. McCall, Appl. Phys. Lett. **32**, 284 (1978).
[2] J. W. Jewell, H. M. Gibbs, S. S. Tarng, A. C. Gossard, and W. Wiegmann, Appl. Phys. Lett. **40**, 29 (1982).

[3] H. A. McKenzie, J. J. E. Reid, H. A. Al-Attar, and E. Abraham, Opt. Commun. **60**, 181 (1986).
[4] Yu. I. Balkarei, A. V. Grigor'yants, Yu. A. Rzhanov, and M. I. Elinson, Opt. Commun. **66**, 161 (1988).
[5] Yu. A. Rzhanov, A. V. Grigor'yants, Yu. I. Balkarei, and M. I. Elinson, Sov. J. Quantum Electron. **20**, 419 (1990).
[6] A. V. Grigor'yants and I. N. Dyuzhikov, Sov. Phys. JETP **74**, 784 (1992).
[7] A. V. Grigor'yants and I. N. Dyuzhikov, Sov. J. Quantum Electron. **24**, 469 (1994).
[8] Special Issue on Information Processing, Appl. Opt. **29**, 1987 (1990).
[9] J. M. Halley and J. E. Midwinter, IEEE J. Quantum Electron. **QE-26**, 348 (1990).
[10] S. T. Ho, S. L. McCall, R. E. Slusher, L. N. Pfeiffer, K. W. West, A. F. Levi, G. E. Blonder, and J. L. Jewell, Appl. Phys. Lett. **57**, 1387 (1990).
[11] Constancy of T_0 means that only the time scales well below the characteristic crystal heating/cooling time are considered throughout, assuming that no change in the lattice temperature occurs during the period of self-pulsations. Practically, this requires that optical excitation is a pulsed one, with a duration of the pulses longer than the period of self-pulsations, but shorter than is necessary to have the crystal temperature changed. These could be the microsecond pulses, which, however, are seen as the (quasi)stationary excitation considering the nanosecond range self-pulsations discussed in the present article.
[12] V. I. Tolstikhin, Tech. Phys. Lett. **19**, 62 (1993).
[13] V. I. Tolstikhin and M. Willander, IEEE J. Quantum Electron. **QE-31**, 814 (1995).
[14] J. L. Merz, R. A. Logan, and A. M. Sergent, J. Appl. Phys. **47**, 1436 (1976).
[15] B. L. Gel'mont, Z. N. Sokolova, and V. B. Khalfin, Sov. Phys. Semicond. **17**, 280 (1983).
[16] S. Adashi, *Physical Properties of III-V Semiconductor Compounds* (Wiley, New York, 1992).
[17] K. Kash and J. Shah, Appl. Phys. Lett. **45**, 401 (1984).
[18] W. Pötz and P. Kocevar, Phys. Rev. B **28**, 7040 (1983).
[19] V. I. Tolstikhin, Sov. Tech. Phys. Lett. **18**, 438 (1992).
[20] *GaInAsP Alloy Semiconductors*, edited by T. P. Persall (Wiley, New York, 1982).
[21] V. I. Tolstikhin and M. Willander, J. Appl. Phys. **77**, 488 (1995).
[22] T. S. Moss, G. J. Burrell, and B. Ellis, *Semiconductor Opto-Electronics* (Butterworths, London, 1973).
[23] V. I. Tolstikhin and M. Willander, Inst. Phys. Conf. Ser. **139**, 597 (1994).
[24] A. A. Andronov, A. A. Vitt, and S. E. Khaikin, *Theory of Oscillators* (Dover, New York, 1987).